Precambrian Research 321 (2019) 212–220

Contents lists available at ScienceDirect

Precambrian Research

journal homepage: www.elsevier.com/locate/precamres

A deep marine organic carbon reservoir in the non-glacial Cryogenian ocean (Nanhua Basin, South China) revealed by organic carbon isotopes

Xi Peng[a,b], Xiang-Kun Zhu[a,*], Fuqiang Shi[a], Bin Yan[a], Feifei Zhang[a], Nina Zhao[a], Pingan Peng[b], Jin Li[a], Dan Wang[a], Graham A. Shields[c]

[a] MNR Key Laboratory of Isotope Geology, MNR Key Laboratory of Deep-Earth Dynamics, Institute of Geology, Chinese Academy of Geological Sciences, Beijing 100037, China
[b] State Key Laboratory of Organic Geochemistry, Guangzhou Institute of Geochemistry, Chinese Academy of Sciences, Guangzhou 510640, China
[c] Department of Earth Sciences, University College London, Gower Street, London WC1E 6BT, UK

ARTICLE INFO

Keywords:
Cryogenian non-glacial interval
Nanhua Basin
Organic carbon isotopes
Organic carbon reservoir
Oxygenation

ABSTRACT

The late-Cryogenian warm (non-glacial) interval (c.660 − c.650 Ma) is potentially of great significance to the co-evolution between life and the surface environment during the emergence of animal life on Earth. In this study, three high-resolution organic carbon isotopic ($\delta^{13}C_{org}$) records for the Datangpo/Xiangmeng Formation on the Yangtze Craton are presented. The data derive from drill cores representing different depositional settings at Daotuo (slope setting), Minle (shallow-water basin), and Xiangtan (basin), respectively. The Daotuo and Minle samples exhibit an overall increase of 6–8‰ as well as significant isotopic fluctuations following the Tiesi'ao/Sturtian glaciation, while samples from the deeper Xiangtan section show relatively muted fluctuations (± 1‰) and no overall trend over the same interval. These findings can be plausibly explained by a much longer residence time for marine organic matter, which may have acted as a redox buffer against oxygenation and climate change. The build-up and eventual oxidation of a sub-pycnocline organic carbon reservoir in the redox stratified non-glacial ocean could help to explain the extreme positive and negative carbon isotope perturbations, respectively, in time-equivalent shallow-marine carbonate Platform successions from Mongolia, Australia and Namibia.

1. Introduction

The Neoproterozoic Era is of great significance in the evolutionary history of the Earth system and life. A series of important geological events occurred during this era, known widely by their evocative nicknames: 'Snowball Earth'; the 'Neoproterozoic Oxygenation Event' (Hoffman et al., 1998; Shields-Zhou and Och, 2011; Sperling et al., 2015). Accompanying these various upheavals was a series of extremely negative perturbations (by as much as 10‰ to 15‰) in the carbon isotopic composition of marine carbonates ($\delta^{13}C_{carb}$), the origin of which is hotly debated (Grotzinger et al., 2011; Johnston et al., 2012; Rose et al., 2012; Schrag et al., 2013). All these hypotheses can be usually divided into primary and non-primary seawater signal hypotheses. The primary seawater signal hypotheses include all organic oxidation hypotheses, e.g., hydrocarbon oxidation (Lee et al., 2015), 'dissolved' organic carbon (DOC) reservoir due to pulsed oxygenation (Rothman et al., 2003; Fike et al., 2006), spatially heterogeneous and partial oxidation of DOC or reduced carbon (Li et al., 2017), decreased primary productivity (Halverson et al., 2002; Knauth and Kennedy, 2009), oxidation of recycled continentally derived organic carbon (Kaufman et al., 2007) and steady C-cycle hypothesis (Johnston et al., 2012). The non-primary seawater signal hypotheses include the diagenetic (Derry, 2010) or authigenic carbonate hypothesis (Schrag et al., 2013).

The behavior that invariant $\delta^{13}C_{org}$ during large changes in $\delta^{13}C_{carb}$ across the Neoproterozoic (1000 to 542 Ma) was thought to result from a very large dissolved organic carbon (DOC) reservoir in the ocean (Rothman et al., 2003). Although this model has received further support by some subsequent studies (Fike et al., 2006; Swanson-Hysell et al., 2010), the existence of organic carbon reservoir in the later Neoproterozoic ocean is still highly controversial (Fike et al., 2006; Bristow and Kennedy, 2008; Swanson-Hysell et al., 2010; Johnston et al., 2012). Much of the emphasis in the later studies for and against organic carbon reservoir has been to examine the relationship between $\delta^{13}C_{carb}$ perturbations and the carbon isotopic composition of organic carbon ($\delta^{13}C_{org}$), in particular whether the two show the same trends or

* Corresponding author.
E-mail address: xiangkun@cags.ac.cn (X.-K. Zhu).

https://doi.org/10.1016/j.precamres.2018.12.013
Received 22 June 2018; Received in revised form 13 December 2018; Accepted 14 December 2018
Available online 16 December 2018
0301-9268/

are decoupled from each other. If $\delta^{13}C_{carb}$ and $\delta^{13}C_{org}$ are coupled, it is suggested that they both formed from the same dissolved inorganic carbon (DIC) reservoir (Johnston et al., 2012). If $\delta^{13}C_{carb}$ and $\delta^{13}C_{org}$ are decoupled, they are both subordinate to the DOC reservoir (Swanson-Hysell et al., 2010). Johnston et al. (2012) carried out a comparative C-isotope study of non-glacial Cryogenian sections from Mongolia, Canada and Namibia. They discovered that data of $\delta^{13}C_{carb}$ and $\delta^{13}C_{org}$ were coupled in F949 section (Mongolia) and P5c section (Canada), but decoupled in P7500 section (Namibia). Johnston et al. (2012) argued that these apparently conflicting results ruled out the existence of the DOC reservoir during the non-glacial Cryogenian ocean. Instead, they proposed a two-component mixing model to explain that the decoupling was the result of admixture of detrital organic carbon, and believed that coupling was the norm in more organic-rich successions. However, the study sections in the Johnston et al. (2012) are all in shallower marine settings. The Cryogenian ocean was not homogeneous (Li et al., 2012; 2017), and the main carbon sources could vary by different depths. Spatial heterogeneity in $\delta^{13}C$ must be considered in models of extremely negative perturbations (Shi et al., 2017, 2018). Thus, the existence of the postulated DOC reservoir has yet to be demonstrated using transects from shallow to deep marine settings.

The existence of an organic carbon reservoir would play a significant role in buffering oxygen levels (Rothman et al., 2003; Fike et al., 2006; Li et al., 2012; Swanson-Hysell et al., 2010). Organic carbon acts as an electron donor in redox reactions, while an organic carbon reservoir could potentially provide enough reductant capacity to sustain ocean redox stratification (Li et al., 2012; Fan et al., 2014). The presence of an organic carbon pool in the ocean would also generate a negative climate feedback, whereby excess organic carbon production would be compensated by a greater net contribution from 'DOC' oxidation, releasing CO_2 and preventing further global cooling and glaciation (Swanson-Hysell et al., 2010). The magnitude and buffering capacity of the putative organic carbon reservoir would be tightly related to the stability and evolution of Earth's surface environment. However, its existence is hotly disputed, with some authors skeptical that enough oxidizing power could ever have been available to remineralise sufficient organic carbon to cause large carbon isotope perturbations (Bristow and Kennedy, 2008). As a result, the precise nature of the organic carbon reservoir is in dispute (Swanson-Hysell et al., 2010; Bjerrum and Canfield, 2011; Johnston et al., 2012), while there is an overall lack of direct geological evidence (Jiang et al., 2012; Johnston et al., 2012). This study attempts to further constrain this important issue by comparing non-glacial Cryogenian carbon isotope profiles of time-equivalent organic-rich successions with different depositional depths.

The Nanhua Basin in South China is a suitable object for this kind of study because of its well-characterized stratigraphic frame work, and its organic-rich nature. The Datangpo Formation and its time-equivalent Xiangmeng Formation were both deposited between the early Cryogenian (Sturtian) glaciation and the late Cryogenian (Marinoan) glaciation in the Nanhua Basin, South China. Three drill cores examined in this study represent the Datangpo/Xiangmeng Formation in its entirety, developed in slope (Daotuo section), shallow-water basin (Minle section), and basin (Xiangtan section) settings (Fig. 1) (Bao et al., 2018).

2. Geological setting and sample descriptions

The Neoproterozoic strata in South China were deposited in a rift to passive margin setting along the southeastern side of the Yangtze Craton (Zhang et al., 2008), and are composed of three major parts (Zhou et al., 2004; Zhang et al., 2008) (Fig. 2B): (1) pre-glacial siliciclastic rocks (Liantuo Formation and Banxi Group);(2) two Cryogenian-aged, glacially-influenced diamictite intervals (Chang'an/Dongshanfeng/Tiesi'ao Formation and Nantuo Formation) that are separated by a manganese-bearing siltstone/shale unit (Datangpo/Xiangmeng Formation); and (3) post-glacial marine carbonates and shales (Doushantuo Formation and Dengying/Liuchapo Formation) that are thick (> 700 m) on the shelf but thinner (< 100 m or even less) in the basin (Zhu et al., 2007). During the Cryogenian, the Yangtze Craton can be divided into three sedimentary facies, representing different depositional environments from northwest to southeast: (1) shelf; (2) slope setting; and (3) basin facies (Bao et al., 2018).

The Datangpo/Xiangmeng Formation is sandwiched between two major glacially-influenced diamictites, the older Tiesi'ao Formation (Gucheng Formation in Hubei Province and western Hunan Province) and the younger Nantuo Formation (Dobrzinski and Bahlburg, 2007; Zhang et al., 2008). The Datangpo Formation and the Xiangmeng Formation are time-equivalent Cryogenian non-glacial (warm interglacial) deposits.

The Tiesi'ao Formation comprises diamictites, and is correlative with Sturtian glacigenic deposits globally (Zhou et al., 2004; Zhu et al., 2007; Macdonald et al., 2010; Zhang et al., 2015). The Nantuo Formation comprises thick diamictites, siltstones, and sandstones, and is correlative with Marinoan glacigenic deposits globally (Condon et al., 2005; Zhang et al., 2005, 2008; 2015, Prave et al., 2016). The Datangpo/Xiangmeng Formation comprise the entire sedimentary record of the Nanhua Basin between the Sturtian and Marinoan glacial intervals.

The Daotuo, Minle and Xiangtan drill cores exhibit different facies and represent different depositional settings (Fig. 1). The Daotuo section is located in Songtao County in northeastern Guizhou Province (N28°07′3.67″, E108°52′25.86″, Drill core ZK105). The Datangpo Formation of the Daotuo section in this drillcore is 240.5 m thick, representing a slope setting. The Minle section is located in Huayuan County in western Hunan Province (Drill core 0905), where the Datangpo Formation is 196.3 m thick, and represents a shallow-water basin setting. The Xiangtan section is located near Xiangtan City in Hunan Province (N27°58′31″, E112°50′22″, Drill core ZK3603), which is 89 m thick and represents a basin setting. The depositional depth of Xiangtan section is deeper than that of Minle section (Fig. 1) (Bao et al., 2018). Although of different thicknesses, the studied sections have a somewhat similar lithologic profile with intervals of manganese carbonate (Figs. 2 and 3), directly overlying Sturtian-age diamictites of the Gucheng or Tiesi'ao formations, followed by organic carbon-rich black shale (or gray-black shale), and/or gray siltstone (Li et al., 2012; Zhang et al., 2015), overlay by Nantuo diamictite. The Datangpo/Xiangmeng Formation exhibits an apparently conformable contact with both the underlying Tiesi'ao/Gucheng Formation and the overlying Nantuo Formation in the studied area (see more details in Section 5.1).

According to lithostratigraphic analysis, the studied Daotuo section can be divided into 5 units (Fig. 2B). Unit 1 is a 0.8-m-thick interval composed of pyritic and organic carbon-rich black shale. Unit 2 is a 12.5-m-thick interval composed of organic carbon and Mn-carbonate shale. Unit 3 is a 38-m-thick interval composed pyritic and organic-rich black shale. Unit 4 is a 145-m-thick gray shale. Unit 5 is a 52.5-m-thick gray siltstone. Detailed lithologic information about the Daotuo section can be found in Zhang et al. (2015). The Datangpo Formation at Minle can be divided into 7 units (Fig. 2B). Unit 1 is a 1.3-m-thick layer composed of pyritic, Mn-carbonate. Unit 2 is a 3.8-m-thick layer composed of gray shale. Unit 3 is a 45.5-m-thick layer composed of black shale. Unit 4 is a 33.0-m-thick layer composed of black shale and gray shale. Unit 5 is a 69.0-m-thick layer composed of gray shale. Unit 6 is a 19.3-m-thick layer composed of black shale, gray shale. Unit 7 is a 24.4-m-thick layer composed of black-silty shale. The Xiangmeng Formation at Xiangtan can be divided into 4 units (Fig. 2B). Unit 1 is a 0.4-m-thick interval composed of Mn-carbonate with organic rich shale. Unit 2 is a 82.0-m-thick interval composed of black shale. Unit 3 is a 1.1-m-thick interval composed of gray-black manganese-bearing limestone. Unit 4 is a 5.5-m-thick interval composed of calcareous, pyritic, gray-black shale.

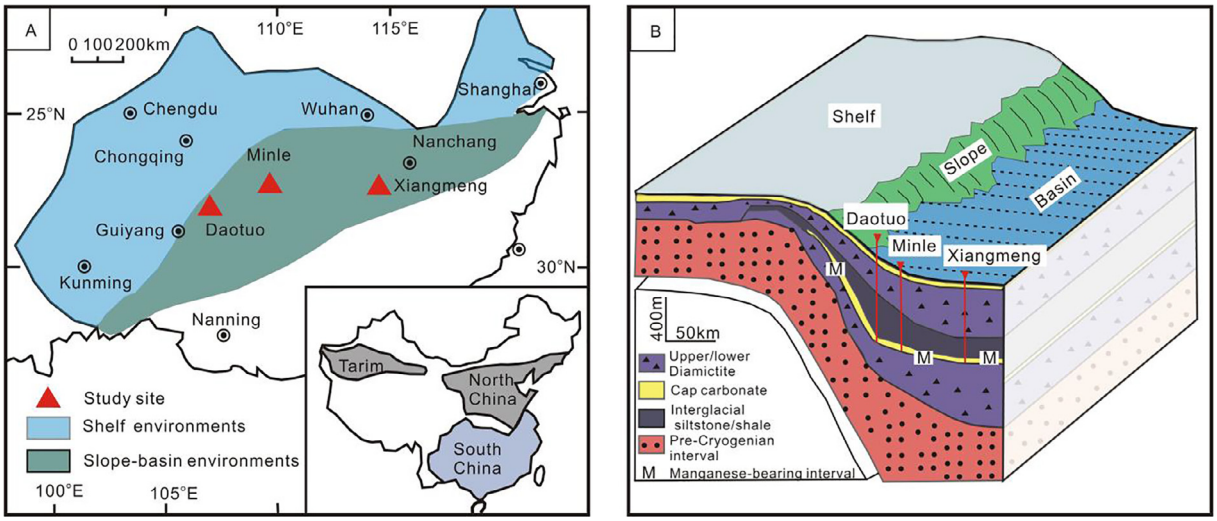

Fig. 1. A simplified paleogeographic map showing the studied area (Bao et al., 2018). (A) Generalized Cryogenian paleogeographic reconstruction of South China. (B) Depositional model showing the paleogeographic position of the studied drillcores.

Looking more widely, the Datangpo Formation and the Taishir Formation in western Mongolia were likely deposited around the same time (Fig. 2A), while the Ombaatjie Formation of Namibia is probably equivalent to the upper portion of the Datangpo Formation (Hoffman, 2011). The Trezona Formation of Adelaide Rift Complex, South Australia is probably equivalent to the upper portion of the Datangpo Formation (Rose et al., 2012).

3. Analytical methods

A total of 456 samples were analyzed for organic C isotope compositions in this study, of which, 231 samples were collected from Daotuo drill core at a spacing of 0.5–2.0 m; 179 samples were collected from Minle drill core at a spacing of 0.1–2.0 m; and 46 samples were collected from Xiangtan section at a spacing of 0.5–4.0 m. For each sample, veins were avoided for every sample to minimise late-stage hydrothermal effects.

For each fresh sample of ca. 3 g was ground to powder (200 mesh) in an automated agate mill. Samples were decalcified with concentrated HCl (6 M) for 1 h at 70 °C, buffered back to about neutral pH (> 5) with deionized water (the wash with deionized water was done 6 times), then centrifuged and the supernatant removed. The siliciclastic content was removed with HF (6 M) for 1 h (70 °C). Samples were then buffered back to about neutral pH (> 5) with deionized water again (the wash with deionized water was done 6 times), centrifuged, and the supernatant removed and evaporated to dryness at 50 °C. Homogenized residues were analyzed on a Vario EL cube elemental analyzer for TOC (total organic carbon) contents, and on a ThermoFinnigan Delta XL Plus in continuous-flow mode for C isotope compositions. External and internal uncertainties were monitored using urea standards, and were better than 0.1% and 0.2‰ for TOC and $\delta^{13}C_{org}$, respectively. To monitor the reproducibility, duplicates were analyzed for every sample. All C isotope compositions are reported as δ values with reference to the Vienna Pee Dee Belemnite standard (V-PDB).

Sample preparation was performed in the MLR Key Laboratory of Isotope Geology, Institute of Geology, Chinese Academy of Geological Sciences, and sample analyses carried out in the State Key Laboratory of Organic Geochemistry, Guangzhou Institute of Geochemistry, Chinese Academy of Sciences.

4. Results

4.1. Daotuo section

The TOC abundances of all the analyzed samples range from 0.01 wt % (at 41 m and 51 m) to 6.35 wt% (at 3.8 m), averaging 0.58 ± 0.92 wt% (n = 230). $\delta^{13}C_{org}$ values range from −33.5‰ (at 4.8 m) to −27.9‰ (at 137 m), averaging −30.6 ± 1.2‰ (n = 230). TOC abundances decrease through the non-glacial interval, from 2.48 wt% to 0.10 wt% (Fig. 5), while $\delta^{13}C_{org}$ values clearly show two successive increasing trends, and an overall increase from −32.3‰ at the base to −29.3‰ at the top. There are also two $\delta^{13}C_{org}$ perturbations (ca. 5‰) at the bottom of the Daotuo section. In Daotuo section, changes in TOC abundances and lithology are not synchronous, and changes in organic carbon isotopes and lithology do not coincide as a whole (Fig. 5).

4.2. Minle section

The TOC abundances range from 0.04 wt% (at 0 m) to 2.67 wt% (at 1.0 m), averaging 0.24 ± 0.31 wt% (n = 179). $\delta^{13}C_{org}$ values range from −33.4‰ (at 14.4 m) to −27.3‰ (at 0 m), averaging −30.3 ± 1.3‰ (n = 179). TOC abundances are higher straight after Sturtian Glaciation than those immediately before Marinoan Glaciation, from 2.67 wt% to 0.11 wt%. And $\delta^{13}C_{org}$ values show an obvious increasing trend during the non-glacial interval, from −32.0‰ to −28.3‰ (Fig. 5). There was a $\delta^{13}C_{org}$ excursion (ca. 4‰) at the bottom of the Minle section. But the change to and away from the nadir is more muted compared with that of the Daotuo section (Fig. 5). For Minle section, TOC abundances and organic carbon isotope values are variable at the bottom and stable for the middle and upper part, while lithology is variable for the whole section (Fig. 5).

4.3. Xiangtan section

The TOC abundances are relatively high, ranging from 0.42 wt% (at 0 m) to 4.80 wt% (at 44.5 m), averaging 3.32 ± 1.16 wt% (n = 46). $\delta^{13}C_{org}$ values range from −34.5‰ (at 0 m) to −31.4‰ (at 70.5 m), averaging −32.6 ± 0.5‰ (n = 46). TOC abundances decrease sharply at 81.5 m, from 2.67 wt% to 0.50 wt% (Fig. 5), but $\delta^{13}C_{org}$ values remain stable through the whole profile, being −32.9‰ at the base and −32.3‰ at the top. Lithology remains unchanged despite the major decrease in TOC near the top of the formation (Fig. 5).

A

Era	Stage	Global glaciation	Eastern Guizhou, China	Northwestern Hunan, China	Tsagaan-olom Basin, Mongolia	Congo Craton, Namibia	Adelaide Rift Complex, Australia
Neoproterozoic	Cryogenian	Marinoan Glaciation	Nantuo Fm. 654.5±3.8 Ma (1)	Nantuo Fm.	Khongor Fm.	Ghaub Fm.	Elatina Fm.
			Datangpo Fm. 662.9±4.3 Ma (2)	Xiangmeng Fm.	Taishir Fm. 659.0±4.5Ma (3)	Ombaatjie Fm.	Trezona Fm.
						Gruis Fm.	
		Sturtian Glaciation	Tiesi'ao Fm.	Gucheng Fm.	Maikhan-Uul Fm.	Rasthof Fm.	Apilla Fm.
			Liangjiehe Fm.	Dieshuihe Fm.	Zavkhan Fm.	Chuos Fm.	

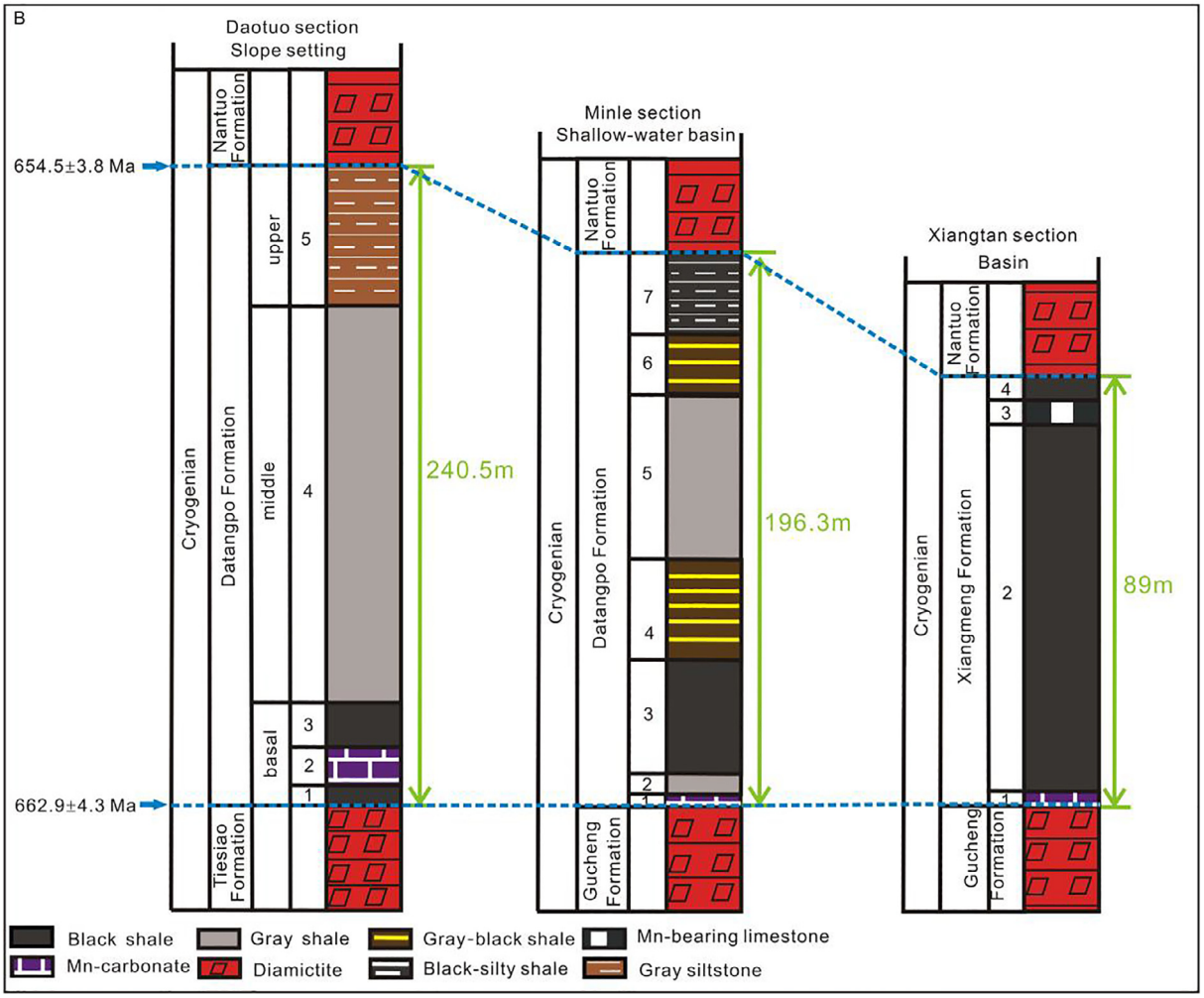

Fig. 2. (A) Stratigraphic correlations of South China and Namibia, Mongolia during Cryogenian non-glacial stage. (B) The stratigraphic column shows the stratigraphic succession of study sections. (1) SHRIMP zircon U-Pb age (Zhang et al., 2008). (2) Zircon U-Pb age (Zhou et al., 2004). (3) Re-Os isochron age (Bold et al., 2015; Rooney et al., 2015).

Although there is no obvious $\delta^{13}C_{org}$ – TOC co-variation in a particular lithology or across the $\delta^{13}C_{org}$ negative perturbations (Fig. 6), strongly negative $\delta^{13}C_{org}$ values are mostly found in black shales with relatively higher TOC abundances.

5. Discussion

5.1. Chronostratigraphic correlation between the three sections

It is generally considered that the Nantuo and the Tie'siao/Gucheng diamititic deposits are equivalent to the global 'Marinoan' and Sturtian glaciations, respectively (Condon et al., 2005; Zhu et al., 2007; Zhang et al., 2008; Prave et al., 2016). Thus, the Datangpo/Xiangmeng Formation covers the whole non-glacial interval between the Cyogenian 'Snowball Earth' events providing there are no stratigraphic hiatus. Therefore, the relative completeness of the studied Datangpo and Xiangmeng formations is vital to interpretations of these isotope data.

It is generally considered that considerable erosion must have occurred across a large area due to the postulated sea-level fall of up to 800 m caused by the 'Marinoan' glaciation (Liu and Peltier, 2013). Indeed, there are differences in thickness and lithology for the three studied sections that might be attributed to erosional truncation. This issue is dealt with specifically below by examining the nature of the contacts between underlying and overlying strata of the studied sections.

5.1.1. Contact relationship with underlying strata

Mn-carbonate ore is a unique feature that is characteristic of the Datangpo/Xiangmeng Formationacross the Yangtze Craton (Fig. 3), and it has been well documented that the Mn-carbonate ore-bearing strata occur at the bottom of the formation (Fan et al., 1992; Zhou et al., 2004; Zhang et al., 2015). As shown in Figs. 2 and 3, Mn-carbonate beds have

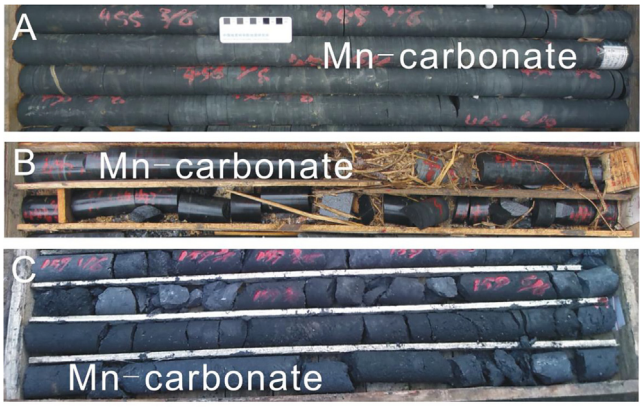

Fig. 3. (A) Strata containing Mn-carbonate ore in the Datangpo Formation for Daotuo section. (B) Strata containing Mn-carbonate ore in the Datangpo Formation for Minle section. (C) Strata containing Mn-carbonate in the Xiangmeng Formation for Xiangtan section.

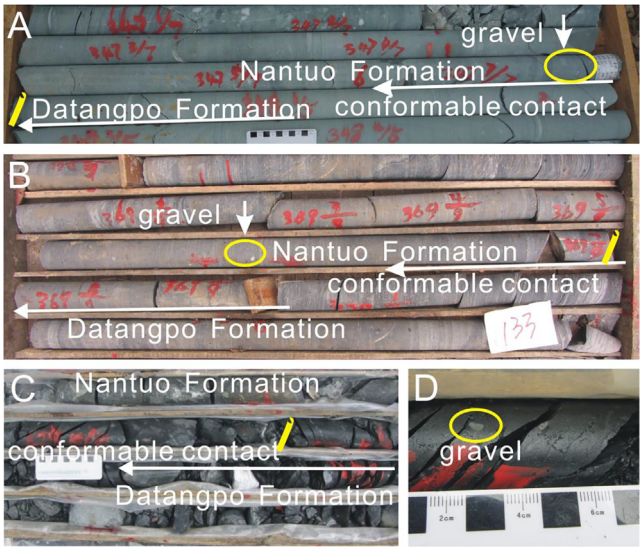

Fig. 4. Drill core photographs. (A) Gradual transition between Datangpo Formation and Nantuo Formation in the Daotuo section, Songtao County in northeastern Guizhou. (B) Gradual transition between Datangpo Formation and Nantuo Formation with the presence in the Minle section, Huayuan County in western Hunan Province. (C) Gradual transition between Datangpo Formation and Nantuo Formation in the Xiangtan section, Xiangtan City in Hunan Province. (D) Gravels in top part of Xiangmeng Formation (black shale) in Xiangtan section.

been observed to mark the base of the non-glacial succession at each of the three localities studied here (Fig. 2). The $\delta^{13}C_{org}$ data are continuous from the Gucheng Formation/Tiesi'ao Formation to the Datangpo Formation in the Daotuo section and Minle section (Fig. 5). These evidences show that the non-glacial sedimentation of the Datangpo/Xiangmeng Formation occurred almost synchronously in the three localities, and that there is no significant hiatus between the non-glacial and underlying glacial sedimentation.

5.1.2. Contact relationship with overlying strata

The base of the Nantuo Formation is marked by the onset of conglomerate (diamictite) deposition (Zhang et al., 2008). Although the transitions between the Datangpo/Xiangmeng Formation and the Nantuo Formation are generally sharp, no discontinuities are observed at any of the three sections (drill cores in the three areas) (Fig. 4). Instead, gradual transitions between the two formations are evident in terms of their colour, organic contents and general lithology (Fig. 4). More importantly, angular gravels have been observed at the top of the Xiangmeng Formation (below the diamictite) in some drill cores (Fig. 4C and D). The large sizes of the angular gravels are in great contrast to those of the host black shale (Fig. 4A–D). Thus, these gravel lonestones are considered to be dropstones. The occurrence of outsized dropstones in otherwise, very fine-grained black shale argues strongly for continuity of sedimentation between the Xiangmeng Formation and the overlying Nantuo diamictite. This rules out any possibility that the Xiangmeng Formation in the Xiangtan area is equivalent only to the black shale part of the Datangpo Formation in the Daotuo area. Furthermore, the $\delta^{13}C_{org}$, TOC data are continuous through the entire Datangpo/Xiangmeng Formation, and from the Datangpo/Xiangmeng Formation to the Nantuo Formation in the Daotuo, Minle and Xiangtan sections (Fig. 5). Therefore, the Xiangtan black shale is considered to cover the entire non-glacial interval in South China, which is consistent with a recent study (Bao et al., 2018).

5.2. Constraints on the depositional settings

Although samples from different depositional settings were purposely selected, using previous studies as a guide, it is important to examine whether features exhibited by the studied samples are consistent with their supposed settings.

5.2.1. Grain sizes

Sediment grain size can reflect hydrodynamic conditions. Coarse grain size is taken to indicate a high energy environment (proximal to terrestrial source), while fine grain size suggests low energy conditions (distal from terrestrial source). Therefore, grain size distribution can reflect sedimentary depth (Ghoshal et al., 2010; Bouchez et al., 2011). The Datangpo Formation at Daotuo is mainly composed of black shale and siltstone, with the portion of siltstone being much larger than that of shale. This is consistent with the Datangpo Formation at Daotuo being situated nearer the land. The Datangpo Formation at Minle is mainly composed of black shale, gray shale and a smaller portion of siltstone, indicating that the depositional site for the Datangpo Formation at Minle was further away from its terrestrial source than for Daotuo, thus likely deeper. The Xiangmeng Formation in Xiangtan is mainly composed of fine black shale, which indicates a quiet depositional environment. Thus, compared with the Datangpo Formation at Daotuo and Minle, the Xiangmeng Formation at Xiangtan was likely deposited in the deepest part of the basin.

5.2.2. Sedimentation rates

The greater thickness of the Datangpo Formation at Daotuo is consistent with the greater abundance of terrestrially-derived material and high sedimentation rates expected of a nearshore environment. Conversely, being most distal from the shore, it is expected that the Xiangmeng Formation at Xiangtan is relatively condensed due to a relative lack of terrestrially-derived material and lower sedimentation rates. The thickness of the Datangpo Formation at Minle is between these two extremes.

Based on grain size and sedimentation rates, we propose that the order of depositional depth for the study sections is: Daotuo < Minle < Xiangtan. This is consistent with previous studies (Fig. 1).

5.3. Temporal and spatial variability of organic carbon isotope composition

Organic carbon isotopic values obtained in this study vary according to depositional setting (Figs. 1 and 5). Firstly, from the nearshore, slope setting to the more distal deep-water basin, average TOC abundances show an obvious increase, from 0.58 wt% to 3.32 wt%; and average $\delta^{13}C_{org}$ values show a significant decrease (Fig. 5), from −30.6‰ to −32.6‰. Secondly, $\delta^{13}C_{org}$ values exhibit an increasing trend with time after the 'Sturtian' glaciation towards the 'Marinoan' glaciation,

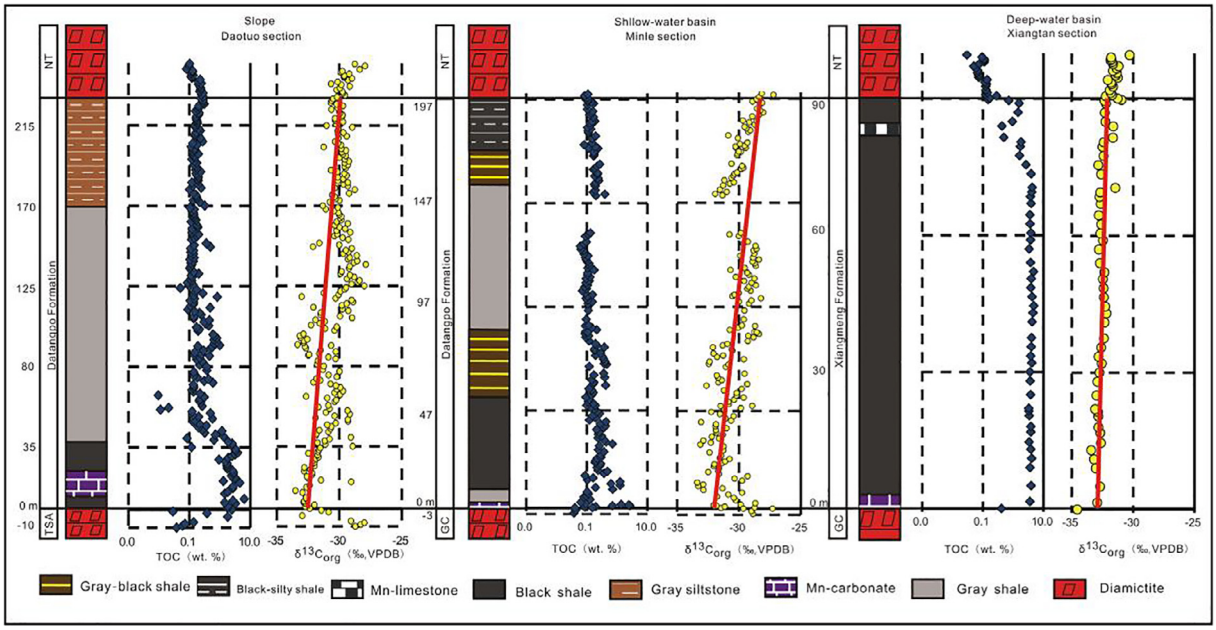

Fig. 5. Spatial and temporal distribution of organic carbon isotopes and TOC abundance. GC denotes the Sturtian-equivalent Gucheng Formation. TSA represents the Sturtian-equivalent Tiesi'ao Formation, and NT represents the Marinoan-equivalent Nantuo Formation.

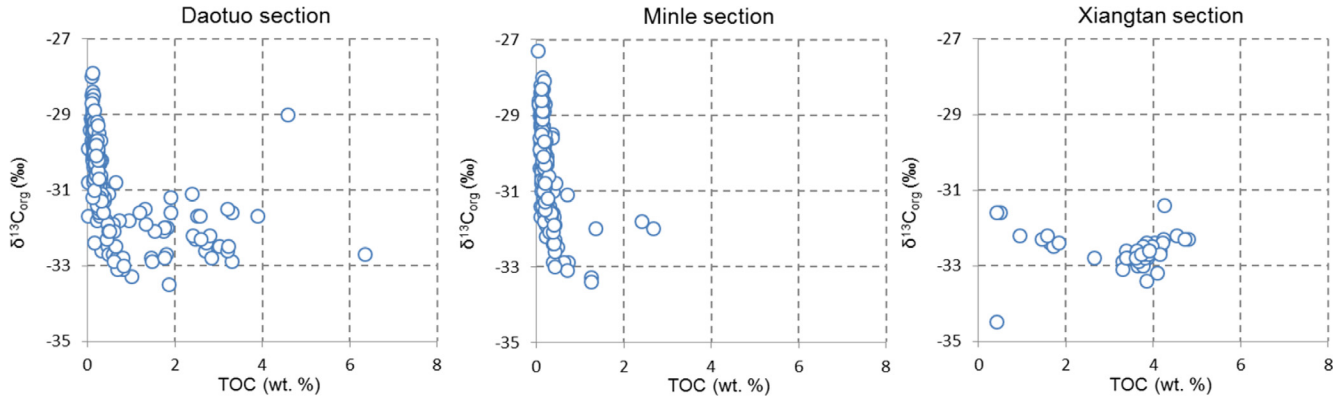

Fig. 6. Crossplots of δ^{13}Corg and TOC abundance for the Datangpo Formation in the Daotuo section and the Minle section, and the Xiangmeng Formation in the Xiangtan section.

especially at Daotuo and Minle. Thirdly, significant negative $\delta^{13}C_{org}$ perturbations are evident in the slope and shallow basin environments: ca. 5‰ at Daotuo and ca. 4‰ at Minle. By contrast, the $\delta^{13}C_{org}$ values at Xiangtan are unchanging. The spatial distribution of $\delta^{13}C_{org}$ values indicates a depth gradient in the isotopic composition of the organic carbon fraction of deposited sediments in the Cryogenian non-glacial warm interval ocean.

5.4. Possible affecting factors for the distributional features of TOC abundance and $\delta^{13}C_{org}$

Besides redox condition, the spatial and temporal distribution of $\delta^{13}C_{org}$ and TOC abundance may be effected by a few factors including: (1) admixture of detrital organic carbon with primary production (Jiang et al., 2012; Johnston et al., 2012); (2) biological pump (Giddings and Wallace, 2009); (3) diagenetic alteration (Giddings and Wallace, 2009; Wang et al., 2016). These possibilities are discussed below.

5.4.1. The effect of detrital organic carbon

Detrital organic carbon, primary production and secondarily recycled primary production (particularly bacteria biomass) are major sources of TOC in marine sediment (Jiang et al., 2012). Terrestrial organic carbon is mainly of low abundance (Burdige, 2007) and so the contribution of detrital carbon in the black shales of the Xiangmeng Formation and lower parts of the Datangpo Formation is unlikely to be significant. Furthermore, the contribution of terrestrial organic carbon would be expected to decrease with increasing distance from the shore. However, TOC abundance at the deeper Xiangtan section is much higher than that at either Daotuo or Minle (Fig. 5). Therefore, it is concluded that the effect of detrital organic carbon is insignificant in our samples, especially in considering the trend of decreasing in TOC with increasing in $\delta^{13}C_{org}$ up section.

5.4.2. Primary productivity and biological pumping

Primary production is controlled by the abundance of nutrients, such as nitrogen and phosphorus. Rivers bring abundant nutrients to the ocean (Bernard et al., 2011), and detrital abundance decreases in general with increasing distance from the shore. Therefore, the contribution that primary producers make to TOC achieves its high point in the slope environment due to the abundant nutrients from terrestrial sources and upwelling waters (Falkowski et al., 1998). This is inconsistent with the observed TOC distribution in our study (Fig. 5).

Biological pumping results from preferential uptake of ^{12}C by

primary producers and remineralization of the ^{12}C-rich organic matter at depth, which leads to shallow DIC enriched in ^{13}C and deep DIC enriched in ^{12}C (Giddings and Wallace, 2009). Biological pumping can cause primary producers at different depths to incorporate dissolved inorganic carbon with different isotope compositions, and this does not necessarily lead to a $\delta^{13}C_{org}$ gradient. In any case, effect from biological pumping cannot explain the temporal trends in $\delta^{13}C_{org}$. Therefore, primary productivity and biological pumping cannot explain the overall organic carbon abundance and $\delta^{13}C_{org}$ distribution.

5.4.3. Early diagenetic alteration and other potential disturbances

Bacterial sulphate reduction and methanogenesis are the main microbially-driven reactions during early diagenesis (Giddings and Wallace, 2009). The intense activity of chemoautotrophic and methanotrophic bacteria can cause $\delta^{13}C_{org}$ values in organic matter to become more negative (Summons et al., 1998; Hollander and Smith, 2001; Jiang et al., 2012). The prerequisites for the activity of chemoautotrophic and methanotrophic bacteria are anoxic conditions and abundant organic matter. Biomass of chemoautotrophic and methanotrophic bacteria could make significant contributions to both the $\delta^{13}C_{org}$ negative shift of the basal part at Daotuo and Minle, as well as the decreasing trend in $\delta^{13}C_{org}$ with depth. However, the activity of chemoautotrophic and methanotrophic bacteria alone cannot explain the overall increasing trend in $\delta^{13}C_{org}$ and/or lack of marked fluctuations in absolute values. Consequently, the effects of early diagenesis are unlikely to be significant for the purposes of our study. In addition, if thermal disturbance, hydrothermal process or other geological alteration occurred, they would change the$\delta^{13}C_{org}$ systematically, but not the overall trends of TOC abundance and $\delta^{13}C_{org}$ in the study sections. Thus, the effect of thermal disturbance, hydrothermal process or other geological alteration would not be discussed in this study.

5.5. A deep marine organic carbon reservoir in a gradually oxygenated ocean

As discussed above, any dominant effect from detrital organic carbon and primary producers on the organic carbon cycle in the studied area can be ruled out. The biological pumping and activity of chemoautotrophic and methanotrophic bacteria rely on abundant organic carbon, and their effects cannot explain the overall $\delta^{13}C_{org}$ trends. In contrast, the existence of a deep marine organic carbon reservoir in a redox-stratified ocean can well explain the temporal and spatial distribution of $\delta^{13}C_{org}$ and TOC abundance. In our study, the deepest depositional environment is associated with greater TOC abundances and more negative $\delta^{13}C_{org}$ values. This organic carbon source is akin to the dissolved organic carbon (DOC) reservoir proposed by Rothman et al. (2003), although the distinction between recalcitrant dissolved and particulate organic matter is not central to the arguments below. It is envisaged that DOC could adsorb on, or aggregate with settling clays in areas of relatively low primary production, thus dominating the organic carbon isotope signature in those settings. The observation that the $\delta^{13}C_{org}$ values at Daotuo, Minle and Xiangtan decrease with depth can be readily explained by the increasing effect of the deep marine organic carbon reservoir at greater depths.

It has been documented that the Cryogenian Nanhua ocean became gradually oxygenated during the Datangpo interval (Li et al., 2012; Zhang et al., 2015). The $\delta^{13}C_{org}$ values at Daotuo and Minle increase with time, which is consistent with the increasing oxidation of organic material due to the increase of seawater oxygenation. It is recalled that light organic is oxidized preferentially. The almost unchanging $\delta^{13}C_{org}$ values for Xiangtan section are due to the deposition occurred below redoxcline and a greater relative contribution from 'old' carbon out of the deep ocean organic carbon reservoir, and is consistent with redox-stratification during most of the late-Cryogenian non-glacial interval in the Nanhua Basin (Shields et al., 1997; Li et al., 2012). The organic carbon is predisposed to build the organic carbon reservoir. As the net growth of the organic reservoir surpassed its peak (high $\delta^{13}C$), and began to oxidize, negative $\delta^{13}C$ anomalies in the shallow marine DIC reservoir and in organic matter produced at shallow depths in the ocean would be predicted to reflect this oxidation.

Small negative shifts in $\delta^{13}C_{org}$ in the basal parts of Daotuo and Xiangtan could have been caused by influx from organic carbon reservoir through ocean upwelling, as for the case documented in the Ediacaran Doushantuo Formation (Fan et al., 2014). Based on the above analysis, it is suggested that there was a large organic carbon reservoir in the Nanhua Basin during the Cryogenian non-glacial interval, and the ocean is gradually oxygenated and redox stratified.

5.6. Is the organic carbon reservoir model of global significance?

The organic carbon reservoir would have helped to buffer oxygen levels on the Earth's surface, and would also have affected the concentration of CO_2 in the atmosphere. Hence, research on the deep marine organic carbon reservoir is critical to exploring the evolutionary history of life and its planetary environment. The opinion of a DOC reservoir existence during the Ediacaran period was mainly based on the decoupling between $\delta^{13}C_{carb}$ and $\delta^{13}C_{org}$ (Fike et al., 2006). Swanson-Hysell et al. (2010) found that there was complete decoupling between $\delta^{13}C_{carb}$ and $\delta^{13}C_{org}$ during the Cryogenian non-glacial interval (C215 and C227 section, being located at Adelaide Rift Complex,

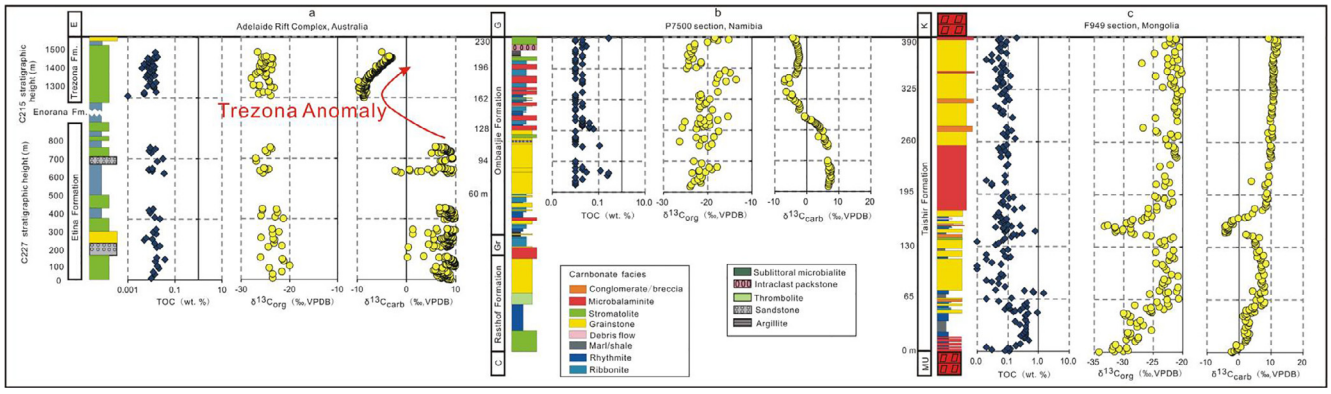

Fig. 7. Spatial and temporal distribution of carbon isotopes and TOC abundance. Data for C215 and C227 section are from Swanson-Hysell et al. (2010). Data for F949 section for the Taishir Formation and P7500 section are from Johnston et al. (2012). C215 and C227 section are located at Adelaide Rift Complex, Australia (31°23′44″S, 138°51′14″E). P7500 section is located at Namibia (19°09′26″S, 13°51′09″E). F949 section is located at Uliastay Gol, Mongolia (46°49′30″N, 95°49′20″E). C indicates the Chuos Formation. E represents the Marinoan-equivalent Etina Formation. G represents the Ghaub Formation, and Gr represents the Gruis Formation. MU represents the Sturtian-equivalent Maikhan-Uul Formation, and K represents the Marinoan-equivalent Khongor Formation.

Australia) (Fig. 7a). Therefore, it was proposed that the huge DOC reservoir had already existed at that time.

However, in a later study, Johnston et al. (2012) found that $\delta^{13}C_{carb}$ and $\delta^{13}C_{org}$ were decoupled in P7500 section (Namibia) (Fig. 7b), coupled in F949 section (Mongolia) (Fig. 7c) and P5c section (Canada). The observation of coupling between $\delta^{13}C_{carb}$ and $\delta^{13}C_{org}$ were thought being not consistent with the DOC reservoir model. Thus Johnston et al. (2012) proposed a quantitative mixing model to explain coupled and decoupled $\delta^{13}C_{carb}$ and $\delta^{13}C_{org}$ data occurred during the Cryogenian non-glacial interval strata, and argued that the apparent conflicting observations ruled out the possibility of the existence of DOC reservoir during the non-glacial Cryogenian ocean.

Using the organic carbon reservoir model proposed in the study, the apparent conflicting observations of coupling and decoupling between $\delta^{13}C_{carb}$ and $\delta^{13}C_{org}$ results can be readily reconciled.

As proposed above, organic carbon reservoir exists in deep basin in a redox stratified ocean. In that case, the effect of organic carbon reservoir on carbon cycling would be generally decreases with the decrease of water depth. In shallow basin settings, the effect of organic carbon reservoir is minimal, and primary producers would be the major organic carbon source. Thus the isotopic compositions of organic and inorganic carbons are coupled, such as those in F949 section, Mongolia (Fig. 7c). In deeper basin settings or environments more prone to seawater upwelling, the effect of organic carbon reservoir would be expected to be more prominent. Thus the isotopic compositions of organic and inorganic carbons may be decoupled, such as in the C215, C227 and P7500 sections (Fig. 7a and b). Therefore, the different relationships between organic and inorganic carbon isotope compositions in different basins can be explained by different effects of organic carbon reservoir, rather than against organic carbon reservoir model.

Whether or not an organic carbon reservoir exists in the Cryogenian ocean is of great significance in term of oceanic and atmospheric redox evolution of the Earth. Further studies are urgently needed to investigate this important issue. At this stage, the evidence believed to be strong against the existence of an organic carbon reservoir is now invalidated.

6. Conclusions

Three complete $\delta^{13}C_{org}$ records for the Datangpo/Xiangmeng Formation representing different depositional settings are presented in this study. The spatial and temporal variability of organic carbon isotopes is in accordance with the existence of a large organic carbon reservoir in the deep sea. The late-Cryogenian non-glacial interval can be viewed as a time when the oceans beneath the pycnocline became rich in organic carbon, which underwent periodic net oxidation under redox-stratified conditions. The existence of an organic carbon reservoir can explain the evolution of organic carbon isotopes in the Dzabkhan Basin, Mongolia and Congo Craton, Namibia as well as Flinders Ranges, South Australia. This study seeks to demonstrate the significance of organic carbon isotopes in building a general framework towards a better understanding of the ocean structure during the Neoproterozoic. Studies of complete, high resolution $\delta^{13}C_{org}$ records in different depositional settings (from slope setting to deep-marine) help us to build a more detailed picture of the carbon cycle and redox conditions in the Nanhua Basin during late-Cryogenian non-glacial, warm interval.

Acknowledgements

This study was financially supported by the Natural Science Foundation of China (Grant No. 41430104), the CAGS research Fund (Grant No. YYWF201603) and the State Key Laboratory of Organic geochemistry Fund (Grant No. OGL-201416). We are grateful to Mr Jiazhuo He and Mr Huashan Chen for their assistance during the determination of TOC abundance and organic carbon isotopic composition. Anonymous reviewers are thanked for their constructive comments.

Appendix A. Supplementary data

Supplementary data to this article can be found online at https://doi.org/10.1016/j.precamres.2018.12.013.

References

Bao, X., Zhang, S., Jiang, G., et al., 2018. Cyclostratigraphic constraints on the duration of the Datangpo Formation and the onset age of the Nantuo (Marinoan) glaciation in South China. Earth Planet. Sci. Lett. 483, 52–63.
Bernard, C.Y., Dürr, H.H., Heinze, C., et al., 2011. Contribution of riverine nutrients to the biogeochemistry of the global ocean-a model study. Biogeoscience 8, 551–564.
Bjerrum, C.J., Canfield, D.E., 2011. Towards a quantitative understanding of the late Neoproterozoic carbon cycle. PNAS 108 (140), 5542–5547.
Bold, U., Macdonald, F.A., Smith, E.F., et al., 2015. Elevating the Neoproterozoic Tsagaan-Olom from Formation to group. Mongolian Geosci. 39, 89–94.
Bouchez, J., Gaillardet, J., France-Lanord, C., et al., 2011. Grain size control of river suspended sediment geochemistry: clues from Amazon River depth profiles. Geochem. Geophys. Geosyst. 12 (3), Q03008.
Bristow, T.F., Kennedy, M.J., 2008. Carbon isotope excursions and the oxidant budget of the Ediacaran atmosphere and ocean. Geology 36, 863–866.
Burdige, D.J., 2007. Preservation of organic matter in marine sediments: controls, mechanisms, and an imbalance in sediment organic carbon budgets? Chem. Rev. 107, 467–485.
Condon, D., Zhu, M., Bowring, S., 2005. U-Pb ages from the Neoproterozoic Doushantuo Formation, China. Science 308, 95–98.
Derry, L.A., 2010. A burial diagenesis origin for the Ediacaran Shuram-Wonoka carbon isotope anomaly. Earth Planet. Sci. Lett. 294, 152–162.
Dobrzinski, N., Bahlburg, H., 2007. Sedimentology and environmental significance of the Cryogenian successions of the Yangtze Platform, South China block. Palaeogeogr. Palaeoclimatol. Palaeoecol. 254, 100–122.
Falkowski, P.G., Barber, R.T., Smetacek, V., 1998. Biogeochemical controls and feedbacks on Ocean Primary Production. Science 281, 200–206.
Fan, D., Liu, T., Ye, J., et al., 1992. The process of formation of manganese carbonate deposits hosted in black shale series. Econ. Geol. 87, 1419–1429.
Fan, H., Zhu, X., Wen, H., et al., 2014. Oxygenation of Ediacaran Ocean recorded by iron isotopes. Geochim. Cosmochim. Acta 140, 80–94.
Fike, D.A., Grotzinger, J.P., Pratt, L.M., et al., 2006. Oxidation of the Ediacaran Ocean. Nature 444 (7), 744–747.
Ghoshal, K., Mazumder, B.S., Purkait, B., et al., 2010. Grain-size distributions of bed load: inferences from flume experiments using heterogeneous sediment bed. Sed. Geol. 223, 1–14.
Giddings, G.A., Wallace, M.W., 2009. Facies-dependent $\delta^{13}C$ variation from a Cryogenian Platform margin, South Australia: evidence for stratified Neoproterozoic oceans? Palaeogeogr. Palaeoclimatol. Palaeoecol. 271, 196–214.
Grotzinger, J.P., Fike, D.A., Fischer, W.W., 2011. Enigmatic origin of the largest-known carbon isotope excursion in Earth's history. Nat. Geosci. 4, 285–292.
Halverson, G.P., Hoffman, P.F., Schrag, D.P., 2002. A major perturbation of the carbon cycle before the Ghaub glaciation (Neoproterozoic) in Namibia: prelude to snowball Earth? Geochem. Geophys. Geosyst. 3 (6), 1035.
Hoffman, P.F., 2011. Strange bedfellows: glacial diamictite and cap carbonate from the Marinoan (635 Ma) glaciation in Namibia. Sedimentology 58, 57–119.
Hoffman, P.F., Kaufman, A.J., Halverson, G.P., et al., 1998. A Neoproterozoic Snowball Earth. Science 281 (5381), 1342–1346.
Hollander, D.J., Smith, M.A., 2001. Microbially mediated carbon cycling as a control on the $\delta^{13}C$ of sedimentary carbon in eutrophic Lake Mendota (USA): new models for interpreting isotopic excursions in the sedimentary record. Geochim. Cosmochim. Acta 65, 4321–4337.
Jiang, G., Wang, X., Shi, X., et al., 2012. The origin of decoupled carbonate and organic carbon isotope signatures in the early Cambrian (ca. 542–520 Ma) Yangtze Platform. Earth Planet. Sci. Lett. 317–318, 96–110.
Johnston, D.T., Macdonald, F.A., Gill, B.C., et al., 2012. Uncovering the Neoproterozoic carbon cycle. Nature 483, 320–323.
Kaufman, A.J., Corsetti, F.A., Varni, M.A., 2007. The effect of rising atmospheric oxygen on carbon and sulfur isotope anomalies in the Neoproterozoic Johnnie Formation, Death Valley, USA. Chem. Geol. 237, 47–63.
Knauth, L.P., Kennedy, M.J., 2009. The late Precambrian greening of the Earth. Nature 460, 728–732.
Lee, C., Love, G.D., Fischer, W.W., et al., 2015. Marine organic matter cycling during the Ediacaran Shuram excursion. Geology 43 (12), 1103–1106.
Li, C., Love, G.D., Lyons, T.W., et al., 2012. Evidence for a redox stratified Cryogenian marine basin, Datangpo Formation, South China. Earth Planet. Sci. Lett. 331–332, 246–256.
Li, C., Hardisty, D.S., Luo, G., et al., 2017. Uncovering the spatial heterogeneity of Ediacaran carbon cycling. Geobiology 15, 211–224.
Liu, Y., Peltier, W.R., 2013. Sea level variations during snowball Earth formation: 1. A preliminary analysis. J. Geophys. Res. -Solid Earth 118, 4410–4424.
Macdonald, F.A., Schmitz, M.D., Crowley, J.L., et al., 2010. Calibrating the cryogenian. Science 327, 1241–1243.
Prave, A.R., Condon, D.J., Hoffmann, K.H., et al., 2016. Duration and nature of the end-Cryogenian (Marinoan) glaciation. Geology 44 (8), 631–634.

Rooney, A.D., Strauss, J.V., Brandon, A.D., 2015. A Cryogenian chronology: two long-lasting synchronous Neoproterozoic glaciations. Geology 43 (5), 459–462.
Rose, C.V., Swanson-Hysell, N.L., Husson, J.M., et al., 2012. Constraints on the origin and relative timing of the Trezona $\delta^{13}C$ anomaly below the end-Cryogenian glaciation. Earth Planet. Sci. Lett. 319–320, 241–250.
Rothman, D.H., Hayes, J.M., Summons, R.E., 2003. Dynamics of the Neoproterozoic carbon cycle. PNAS 100 (14), 8124–8129.
Schrag, D.P., Higgins, J.A., Macdonald, F.A., et al., 2013. Authigenic carbonate and the history of the global carbon cycle. Science 339, 540–543.
Shi, W., Li, C., Algeo, T.J., 2017. Quantitative model evaluation of organic carbon oxidation hypotheses for the Ediacaran Shuram carbon isotopic excursion. Sci. China Earth Sci. 60, 2118–2127.
Shi, W., Li, C., Luo, G., et al., 2018. Sulfur isotope evidence for transient marine-shelf oxidation during the Ediacaran Shuram Excursion. Geology 46, 267–270.
Shields, G.A., Stille, P., Brasier, M., Atudorei, N.-V., 1997. Stratified oceans and oxygenation of the late Precambrian. Terra Nova 9, 218–222.
Shields-Zhou, G.A., Och, L., 2011. The case for a Neoproterozoic oxygenation event: geochemical evidence and biological consequences. GSA Today 21 (3), 4–11.
Sperling, E.A., Wolock, C.J., Morgan, A.S., et al., 2015. Statistical analysis of iron geochemical data suggests limited late Proterozoic oxygenation. Nature 523 (23), 451–454.
Summons, R.E., Franzmann, P.D., Nichols, P.D., 1998. Carbon isotopic fractionation associated with methylotrophic methanogenesis. Org. Geochem. 28 (7–8), 465–475.
Swanson-Hysell, N.L., Rose, C.V., Calmet, C.C., et al., 2010. Cryogenian Glaciation and the onset of carbon-isotope decoupling. Science 30 (328), 608–611.
Wang, X., Jiang, G., Shi, X., et al., 2016. Paired carbonate and organic carbon isotope variations of the Ediacaran Doushantuo Formation from an upper slope section at Siduping, South China. Precambr. Res. 273, 53–66.
Zhang, S., Jiang, G., Zhang, J., et al., 2005. U-Pb sensitive high-resolution ion microprobe ages from the Doushantuo Formation in South China: constraints on late Neoproterozoic glaciations. Geology 33 (6), 473–476.
Zhang, S., Jiang, G., Han, Y., 2008. The age of the Nantuo Formation and Nantuo glaciation in South China. Terra Nova 20 (4), 289–294.
Zhang, F., Zhu, X., Yan, B., et al., 2015. Oxygenation of a Cryogenian ocean (Nanhua Basin, South China) revealed by pyrite Fe isotope compositions. Earth Planet. Sci. Lett. 429, 11–19.
Zhou, C., Tucker, R., Xiao, S., et al., 2004. New constraints on the ages of Neoproterozoic glaciations in south China. Geology 32 (5), 437–440.
Zhu, M., Zhang, J., Yang, A., et al., 2007. Integrated Ediacaran (Sinian) chronostratigraphy of South China. Palaeogeogr. Palaeoclimatol. Palaeoecol. 254, 7–61.